

Fluorescent Nanoprobes with Oriented Modified Antibodies to Improve Lateral Flow Immunoassay of Cardiac Troponin I

Doudou Lou,[†] Lin Fan,[†] Yan Cui,[‡] Yefei Zhu,[§] Ning Gu,^{*,†} and Yu Zhang^{*,†}

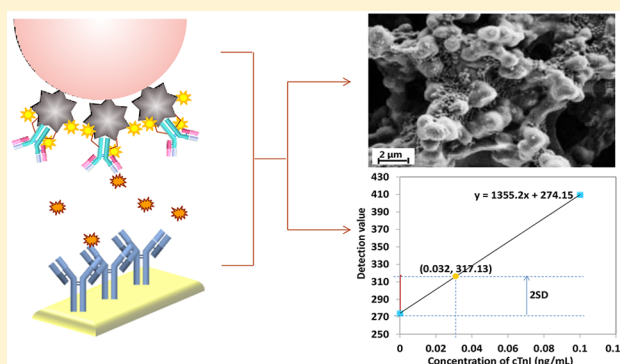
[†]State Key Laboratory of Bioelectronics, Jiangsu Key Laboratory for Biomaterials and Devices, School of Biological Science and Medical Engineering and Collaborative Innovation Center of Suzhou Nano Science and Technology, Southeast University, Nanjing, People's Republic of China

[‡]Nanjing Nanoeast Biotech Co., Ltd., Nanjing, People's Republic of China

[§]Laboratory Medicine Center, The Second Affiliated Hospital of Nanjing Medical University, Nanjing, People's Republic of China

Supporting Information

ABSTRACT: Performance of nanoprobes can often determine the detection level of Lateral immunochromatography. Traditional probes were limited by the quantity and orientation of antibodies, immune activity of the Fab region or binding strength between protein and substrate. This study developed a new efficient and robust technology to construct fluorescent nanoprobes with oriented modified antibodies, based on specific binding of the Fc region of antibody with streptococcal protein G (SPG) on the surface of polystyrene microspheres (MS) and subsequent covalent cross-linking at binding sites to firm them. Lateral flow immunoassay using these probes was applied for the detection of cardiac troponin I (cTnI). The significantly improved detection sensitivity demonstrated that antibody orientation on MS surfaces effectively enhanced immunological activities of probes compared with random immobilizing methods. Furthermore, performance evaluation results of lateral flow test strips met clinical requirements perfectly, including limit of detection (0.032 ng/mL), linearity ($R > 0.99$), repeatability ($CV < 10\%$), correlation ($R > 0.99$), and heat aging stability. This research also employed heterophilic blocking reagent (HBR) to actively block redundant binding sites of SPG for the first time in order to eliminate false positive interferences, improving the sensitivity and precision of test results further.



Lateral immunochromatography is a new immunoassay technology with the unique advantages of being simple, rapid, accurate, portable, and pollution-free. Lateral flow test strips are widely applied to in vitro diagnosis (IVD),¹ environment monitoring,² and food security³ fields since invented, especially developing rapidly in point-of-care testing (POCT)⁴ in recent years, which brings higher requirements on sensitivity and quantitative detection capability. Fluorescent reagents are sensitive, stable, and easy to quantify, gradually replacing traditional gold nanoparticles, becoming one of the most popular signal sensing materials.

The construction approach of fluorescent nanoprobes can often determine the detection level of test strips. In a general way, antibodies and fluorophores are loaded on nanoparticles directly. It is noteworthy that the quantity and orientation of antibodies, immune activity of the Fab region, and binding strength between antibodies and nanoparticles are key elements affecting the bioactivity of probes, which have important influences on the sensitivity and specificity of test results.^{5,6}

Passive adsorption and covalent coupling are two major traditional approaches to load antibodies onto nanoparticles (Figure 1a,b). In the passive adsorption method, antibodies load on substrate mainly through hydrophobic interactions and

electrostatic forces,⁷ being easily affected by antibody isoelectric point, hydrophobic group distribution, temperature, ionic concentration, and lots of others factors, which makes it impossible to obtain an optimized, universal reaction condition.⁸ Furthermore, the reversible adsorption is not stable enough for the quality control of the probes.

In covalent coupling method, carboxyl groups on MS are activated first, then conjugated with antibodies chemically.⁹ The antibody binding quantity and strength increase, but covalent bonds randomly occupy active amino groups of antibodies, so there is a great possibility that the antibody activity is weakened by the occupied groups near or on the antigen binding domains due to steric hindrance. Some other researchers add sandwich layers between MS and antibodies. For example, probes can be constructed by conjugating streptavidin-coated MS with biotinylated antibodies (Figure 1c).¹⁰ Most of these methods require the antibody to be pretreated, which usually leads to antibody denaturation and reduces antigen binding activity.

Received: December 25, 2017

Accepted: April 26, 2018

Published: April 26, 2018

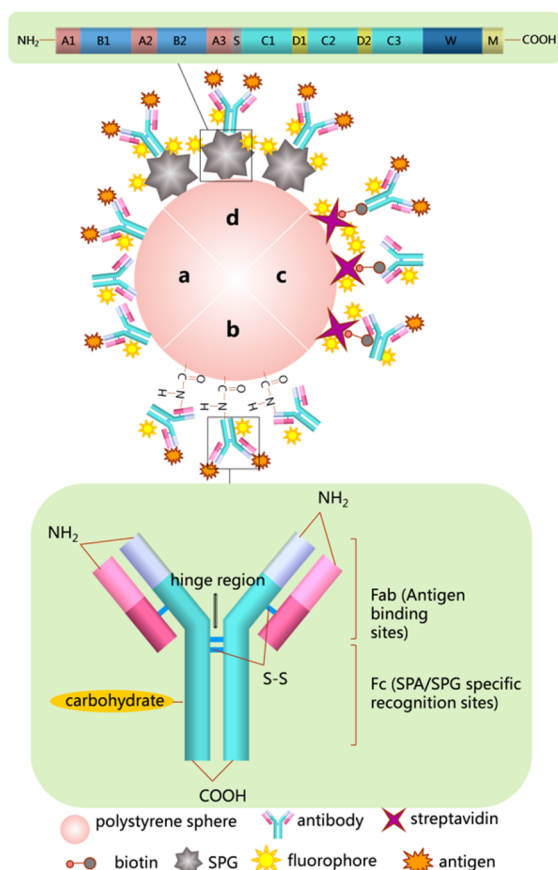


Figure 1. Approaches to load antibodies onto nanoparticles: passive adsorption (a); covalent coupling (b); streptavidin–biotin conjugation (c); SPG orientation (d).

In all the above methods, antibodies are immobilized randomly. As a result, the Fab region partially or completely loses its access to antigens.^{11,12}

Studies on antibody orientation usually focus on loading antibodies on carriers firmly with appropriate density, expose Fab domains sufficiently and protect their bioactivity. In common orientation methodologies, disulfide bonds at the hinge region^{13,14} and carbohydrates at the Fc region^{15,16} are mostly used as binding sites (the bottom inset of Figure 1). However, antibodies have to be preprocessed to reduce disulfide bonds to thiols or oxidize oligose to obtain aldehyde groups. In this case, reaction conditions are difficult to control and over reduction or oxidation occurs easily, reducing the activity of antibodies.

Polypeptides and proteins such as staphylococcal protein A (SPA)^{17,18} and streptococcal protein G (SPG)^{19,20} are also employed as a sandwich layer, targeting the Fc region directly with bioaffinity (Figure 1d). Antibodies do not need to be pretreated and are captured site-directed, which preserves antigen binding activity perfectly and exposes Fab domains sufficiently. Compared with SPA, the C1~C3 domains of SPG (the top inset of Figure 1) have stronger specificity to the Fc region of most subtypes of various animal antibodies, especially to all the subtypes of murine antibodies, which are most commonly used in the immunodetection field.^{21,22} However, this kind of combination is reversible and the affinity strength is affected by the types of antibodies. SPA and SPG are widely used in antibody purification because combination and dissociation procedures are both easy to operate, but

preparation of probes and lateral flow immunoassay require a firmer immobilization strength between antibodies and substrates, otherwise extreme conditions like centrifugal washing repeatedly, drying treatment, and long-term storage can easily cause antibodies to fall off and lose activity.

Antibody oriented modification can be also realized with protein fusion,²³ molecular imprinting,²⁴ and so on; however, their disadvantages in nonuniversality, high-cost, and complexity make these methods difficult to be applied outside the lab.

It should be noted that the majority of antibody oriented research achievements are based on planar and smooth two-dimensional sensor supports up to now. The significance of antibody orientation on three-dimensional supports such as nitrocellulose membrane, porous gel and MS remains controversial and only a few researches focus on the construction of antibody oriented modified nanoprobe.²⁵ Less work use protein A or G to orient antibodies on three-dimensional supports and rarely use cross-linkers for immobilization. Besides, studies on three-dimensional supports indicate that not all this kind of antibody orientation methods lead to better results. Planar supports have smaller surface and simpler morphology, but it is more difficult to evaluate the role of antibody orientation on complicated three-dimensional surfaces.

In this study, we constructed fluorescent nanoprobe with oriented antibodies based on the Fc specificity of SPG. The Fc region of anti-cTnI antibody was captured by the C1~C3 domain of SPG, then chemically bonded to SPG by carbodiimide (EDC). Through this efficient way, antibodies were oriented immobilized on MS substrates robustly and the Fab region exposed sufficiently, maximally preserving the immune activity. The probes were applied in lateral flow immunoassay to detect human cardiac troponin I (cTnI), an important myocardial damage marker, to improve the detection sensitivity and the storage stability. Heterophilic blocking reagent (HBR) was used as a SPG blocking agent for the first time, to further improve the specificity of detection results.

EXPERIMENTAL SECTION

Construction of Nanoprobes. In the passive adsorption method (control group 1), 500 μg of unmodified MS (Nanoeast) were dispersed in MES buffer (50 mM, pH 5.0), then 100 μg of antibody clone 3H9 (OriGene) was added and incubated for 4 h. After centrifugal washing, the supernatant was pipetted and discarded, then 2% of BSA (Yeason) solution was sufficiently mixed with the deposit and incubated for 30 min to block redundant sites. After centrifugal washing, 10 μg of alexa fluor 647 NHS ester (F647; Thermo Fisher) was mixed with the deposit and incubated for 2 h. The reaction product was centrifugal washed twice and dispersed in glycine buffer (0.05 mM, pH 8.5) containing casein (Sigma-Aldrich) and sucrose (Sinopharm) as protective agents. All the incubation steps were conducted in a horizontal shaker (Topscien). In the covalent coupling method (control group 2), 500 μg of carboxyl-modified MS (JSR) were dispersed in MES buffer (50 mM, pH 5), then 120 μg of EDC (Sigma-Aldrich) and 120 μg of Sulfo-NHS (Sigma-Aldrich) were added and incubated for 45 min. After centrifugal washing, 100 μg of antibody clone 3H9 was mixed with the deposit and incubated for 4 h. Then the BSA blocking and F647 incubation procedures were the same as above. In the SPG orientation method (control group 3), 500 μg of carboxyl-modified MS were dispersed in MES buffer (50 mM, pH 5), then 120 μg of EDC and 120 μg of

Sulfo-NHS were added and incubated for 45 min. After centrifugal washing, 100 μg of SPG (Bioworld) was mixed with the deposit and incubated for 4 h. After centrifugal washing, 100 μg of antibody clone 3H9 was mixed with the MS-SPG compound deposit and incubated for 4 h. Then the BSA blocking and F647 incubation procedures were same as above. Unless otherwise specified, all SPG mentioned were native ones. In SPG orientation and cross-linker immobilization method (the experimental group), 500 μg of carboxyl-modified MS were dispersed in MES buffer (50 mM, pH 5), then 120 μg of EDC and 120 μg of Sulfo-NHS were added and incubated for 45 min. After centrifugal washing, 100 μg of SPG was mixed with the deposit and incubated for 4 h. After centrifugal washing, 100 μg of antibody clone 3H9 was mixed with the MS-SPG compound deposit and incubated for 4 h, then 120 μg of EDC was added into the reaction system and incubated for 4 h, in order to form covalent bond and enhance binding strength between the Fc region and SPG. Then the BSA blocking and F647 incubation procedures were same as above.

Fabrication of cTnI Quantitative Test Strips. The test line and control line were drawn with antibody clone TP-110 (OriGene; 2 mg/mL dispersed in phosphate buffer, pH 7.4, at a speed of 0.8 $\mu\text{L}/\text{cm}$) and goat antimouse polyclonal antibody (Sigma-Aldrich; 0.5 mg/mL dispersed in tris buffer, pH 7.4, at a speed of 0.8 $\mu\text{L}/\text{cm}$), respectively, on nitrocellulose membrane (NC membrane; Merck) with a interval of 3 mm. Sample pads and conjugation pads were treated with solution containing multiple protective and blocking agents, then probes (density of MS was 2 mg/mL) were sprayed on the conjugation pad at a speed of 2.5 $\mu\text{L}/\text{cm}$. All the components were air-dried at room temperature for at least 24 h and attached on the back plates successively, cut into 4 mm wide strips, and stored at room temperature in a dry environment.

Optimization of Antibody Binding pH with SPG. After combining with SPG, MS were dispersed in buffers of different pH values (pH 4, 5, 6, and 7), incubated with antibody clone 3H9 and EDC in sequence. The effects of pH value to the probes and detection results were compared.

Optimization of Probe Blocking Method with HBR. BSA was the most commonly used blocking agent in nanotechnology,^{26,27} which worked in a nonspecific and passive way, thus, it was improbable to block all the extra active sites of SPG. The exposed active sites of SPG can target antibodies on the test line directly and lead to false positive reading, reducing the sensitivity and specificity of test results.

In addition to BSA, HBR (Genstars) was added to the sample pad treatment solution, 12 mg of HBR per pad (20 cm \times 30 cm). In order to determine the effects of HBR, test strips with or without HBR were used to detect samples with cTnI concentrations of 0.1 and 0 ng/mL. Each sample was tested three times. After that, samples containing 0.5 ng/mL of cTnI were detected 10 times with these two kind of strips separately, calculating the coefficient of variation (CV).

Comparison of Native and Recombinant SPG. Two different types of SPG were used to construct probes, one of which was native SPG from the streptococcus cell wall, and the other was recombinant SPG expressed in *E. coli*. The binding efficiency of proteins on MS substrates and the immune activity of probes were determined by micro BCA protein assay kits (Thermo Fisher) and cTnI detection results, respectively.

Characterization of Probes and Test Strips. Dynamic Light Scattering (DLS; Malvern) was used to measure hydrodynamic sizes of unmodified MS, SPG modified MS,

and the final probes. BCA kit was used to determine the binding efficiency and binding strength of proteins. UV-vis spectrophotometer (Shimadzu) and laser confocal microscope (Leica) were used to characterize fluorophores on probes. Scanning electron microscope (SEM; Zeiss) was used to characterize MS and the surface microstructure of the test line region before and after assay.

Immunoassay Procedure and Performance Evaluation of Test Strips. A total of 100 μL of sample solution was added onto the sample pad of a strip and incubated for 15 min. Fluorescent quantitative immunoassay analyzer was used to scan, read, and record fluorescent signal value. Then linearity, repeatability, and limit of detection (LOD) of strips were analyzed and evaluated. Strips were accelerated aged at 37 $^{\circ}\text{C}$ for 30 days,^{28,29} then linearity and repeatability were compared with freshly made strips, assessing the storage stability of strips.

Besides, 31 clinical human serum samples were collected and detected with test strips after they were detected by Beckman-Coulter automatic biochemical analyzer. The results of both systems were compared and a correlation analysis was carried out.

RESULTS AND DISCUSSION

Comparison of Different Probe Construction Methods. MS with a diameter of 240 nm was used in this research due to its great performance in detection sensitivity, specificity, and clean background (Figures S1 and S2). In the whole probe construction process of the experimental group, the polydispersity index (PDI) kept lower than 0.3, indicating that the mild reaction condition guaranteed good monodispersity of the MS-protein conjugates, which was an important foundation to obtain surface homogeneous probes and to get stable detection results. The hydrodynamic sizes of unmodified MS, SPG-modified MS, and the final probes were 220, 245, and 267 nm, respectively, increasing with the coating of proteins. The BCA detection results showed that there were 140 μg of SPG conjugated on the surface of 1 mg of MS, meaning the coupling efficiency was 70%. Then 170–180 μg of antibodies were captured by the MS-SPG conjugates; thus, each antibody occupied about 35 nm^2 on the surface of MS, which was nearly equal to the area an antibody occupied when the Fc was substrate facing (end-on).⁶ It was reasonable to assume that antibodies formed a dense layer on the surface in a “end-on” way. In this case, we inferred the cross-linking reaction mostly occurred in two ways: one was in Fc-SPG contact sites as we expected, another was between antibody neighbor side chains which had little impact on Fab's activity and could also help to maintain the probe conformation.

The binding efficiency and stability of MS-antibody/MS-SPG-antibody compounds using different methods were characterized (Figure 2a, BCA kit detection results). The initial binding efficiencies were sorted in ascending order: passive adsorption \approx covalent coupling < SPG orientation \approx SPG orientation and cross-linker immobilization. All the four groups of probes in solution were stored for 5 days at 4 $^{\circ}\text{C}$ refrigerator and then centrifuged. The supernatants were collected and detected by BCA kit to quantify antibodies fell off from MS. There were about 32% of antibodies falling off to the supernatant in passive adsorption group and 22% for SPG orientation group. Meanwhile, for covalent coupling and SPG orientation and cross-linking groups, antibodies were hardly detectable in the supernatants. This phenomenon proved that SPG had a strong affinity for antibodies and could rapidly

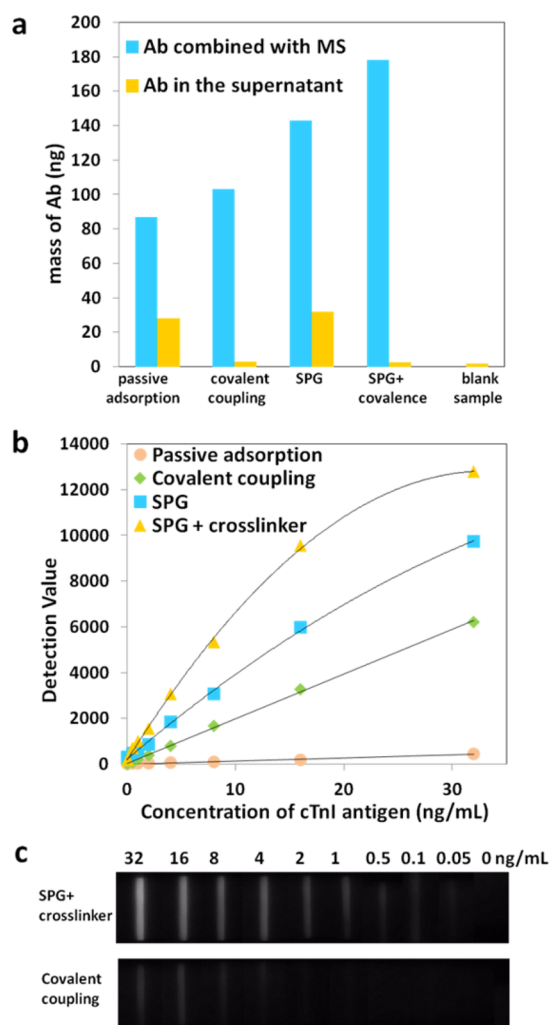


Figure 2. Characterization of probes prepared with different methods: mass of antibodies combined with MS and fell off into supernatant after 5 days (a); gradient cTnI detection results (b); and fluorescent photographs (c).

combine with more antibodies than traditional physical or chemical methods. Unfortunately, the combination strength was not good enough, so that both centrifugal washing and mild short-term storage could lead to antibodies detachment. By using proper cross-linking agent as “adhesive”, the immobilization of antibodies on SPG was reinforced perfectly.

The high antigen binding capacity of the experimental group was demonstrated by using four groups of probes to fabricate test strips and detect cTnI samples (Figure 2b). The fluorescent signal intensities of all the groups strengthened with the increase of cTnI concentrations, showing good gradients. However, it was obvious that the detection values of the experimental group were higher than those of the control groups, which meant the sensitivity was improved by the SPG orientation and cross-linker immobilization method. Fluorescent photographs in Figure 2c could also prove it. In this research, the activity of probes was mainly affected by the total quantity of antibodies and the exposing degree of Fab terminals. After unifying the quantity of antibodies immobilized on different kind of probes, the experimental group still had the highest bioactivity and sensitivity (Figure S3). Therefore, more Fab terminals of the experimental group exposed into the solution, in other words, more Fab regions were oriented

outward than control groups. In a word, the experimental group not only immobilized more antibodies but also exposed the Fab terminals more sufficiently.

Optimized pH of SPG Combining Antibody Procedure. According to the BCA detection results, the combination quantity of antibodies onto MS-SPG was barely effected by reaction pH. Binding efficiencies in reaction conditions of pH 4, 5, 6, and 7 were, respectively, 82.6%, 87.0%, 80.3%, and 80.2% before EDC treatment and 83.5%, 86.7%, 80.0%, and 82.2% after that, having almost no change. The effects of reaction pH and EDC treatment on antibody modified quantity were both much lower than expected, which might be due to the inherent high binding efficiency between antibodies and SPG.

The corresponding four groups of test strips using probes with different reaction pH values were evaluated by comparing their detection gradients and sensitivities subsequently. Samples of gradient cTnI concentrations were detected and the results were analyzed. As shown in Figure 3a, signal values of each group showed good gradients, while signal strengths of groups pH 4 and 5 were much higher than those of groups pH 6 and 7. Therefore, the optimized SPG-antibody reaction pH was at 4 to 5. Previous studies also showed that the maximal antibody binding efficiency of SPG was at pH 4 and 5.³⁰

Optimization of Probe Blocking Method with HBR. Heterophilic antibodies in human serum samples are capable to cross-link the capture and the detection murine antibodies, leading to false positive results.³¹ HBR contains specific murine immunoglobulins and other components which are routinely used to block the heterophilic interaction in immunoassay by active or passive blocking the heterophilic antibodies, thereby eliminating the undesirable interferences. Very similar to the mechanism of heterophilic antibodies, SPG are capable to choicelessly target the Fc region of various antibodies too. In the process of detection, there probably existed exposed sites of SPG on the probes due to incomplete passive blocking of BSA. These SPG easily targeted antibodies coated on the test line directly and the false positive readings appeared then. For this reason, HBR was used as the enhanced blocking reagent during chromatographic process (Figure 3b,c). After treated with HBR, samples of cTnI using bovine serum as matrix were tested. As shown in Figure 3b, the detection values decreased overall but the distinguish extent between 0.1 and 0 ng/mL significantly improved. Additionally, the CV of 0.5 ng/mL sample detection results decreased to 7.8%, while the value was up to 26.7% without HBR. In summary, with HBR treatment, the false positive disturbances were suppressed, further improving the sensitivity and the precision of test results.

Comparison of Native SPG and Recombinant SPG. Native whole SPG and SPG fragments with molecular weight greater than 35KD can recognize not only Fc domains but also Fab domains of murine antibodies. Although the affinity for the Fab region has been proved to be 10-fold lower than Fc region, it may still result in adverse effects.³² Based on the probe construction method in this research, the almost complete native SPG (58KD) and the recombinant SPG reserving only C1~C3 domains (22.4KD) were compared. The BCA test results showed that 1 mg of MS could bind about 137.5 μ g of native SPG and 34 μ g of recombinant SPG respectively, meaning that the numbers of native SPG were 1.6-fold higher than recombinant ones. Subsequently, the antibody binding capacity of both MS-SPG complexes were tested. The captured antibody quantities were 165.7 μ g and 112.7 μ g respectively, corresponding to numbers of SPG. It indicated that native SPG

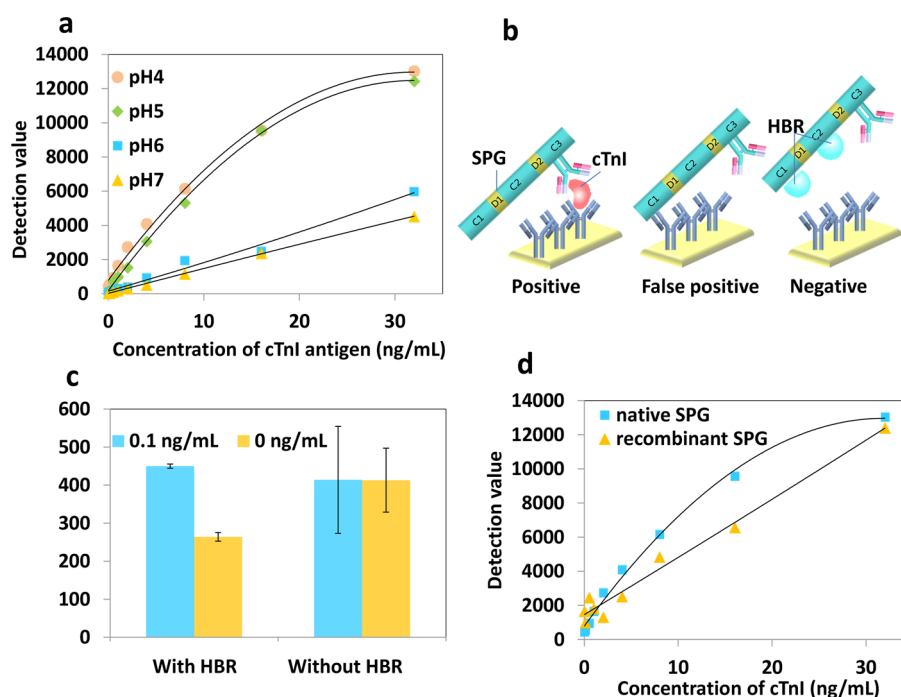


Figure 3. Optimization of probes on the aspects of Ab-SPG binding pH (a); HBR as enhanced blocking reagent (b, c); selecting the optimal SPG as the sandwich layer (d).

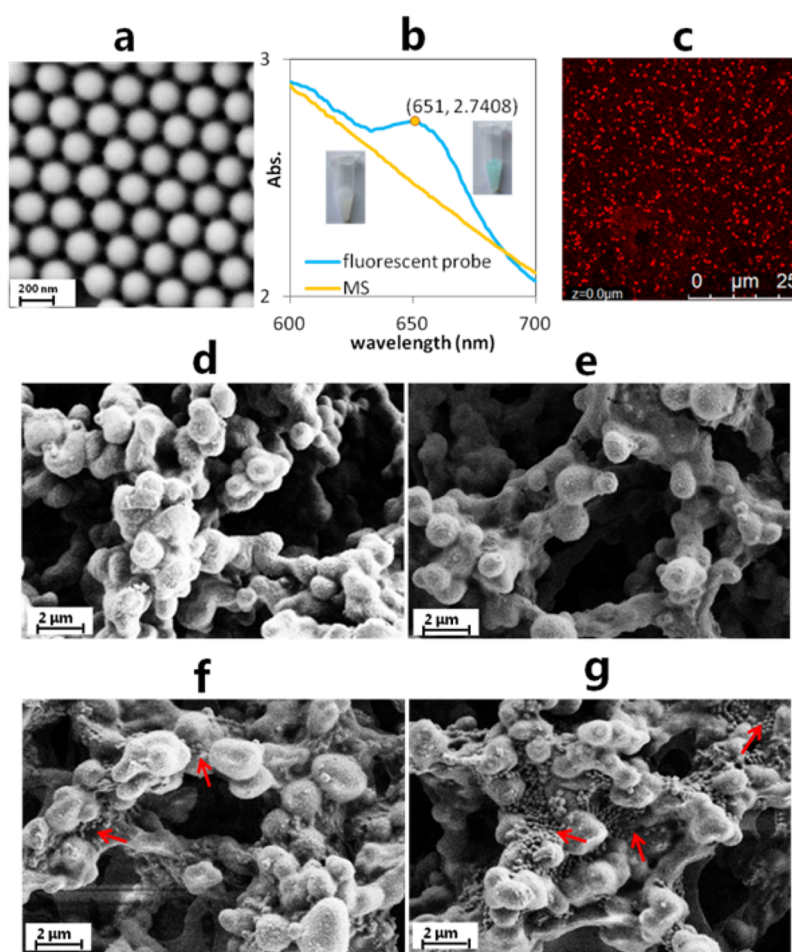


Figure 4. SEM image of MS (a); UV-vis absorption spectra of naked MS and probes (b); fluorescent image of probes (c); and SEM images of blank nitrocellulose membrane (d), membrane after analysis of cTnI negative sample (e), membrane after analysis of cTnI weakly positive (0.5 ng/mL) sample (f), and membrane after analysis of cTnI strongly positive (32 ng/mL) sample (g).

was easier to bind to MS, thus leading to higher antibody binding efficiency, which might be due to larger SPG molecules carried more amino groups so that they had more opportunity to be captured by activated carboxyl groups on MS.

Strips of native and recombinant groups were tested and analyzed (Figure 3d), respectively. On the whole, the gradient relationship between concentrations and signal strengths of recombinant SPG strips were unsatisfactory, especially in low concentration region. More than that, its false positive reading of the negative sample was much higher than the native SPG strip, which could not be eliminated by BSA or HBR blocking.

Characterization and Performance Evaluation of Nanoprobes and Test Strips. The MS used in this research had uniform size and regular shape (Figure 4a). After fluorescent labeling, the color of MS turned blue, appearing a absorption peak at 651 nm (Figure 4b), which was consistent with the characteristic absorption peak of F647. The fluorescent image of probes indicated that probes could produced strong fluorescent intensity and dispersed well (Figure 4c).

After cTnI detection, the used optimized strips were air-dried for 24 h and characterized by SEM. Figure 4d showed that the surface of the NC membrane was a porous network structure providing huge surface area, which was superior to the smooth two-dimensional sensors because of the excellent ability to contact and bear many more probes. Micron-sized holes were able to let probes pass smoothly. Therefore, when the cTnI negative sample was tested, there was little nonspecific adsorption of probes left on NC membrane (Figure 4e). With the increase of cTnI concentration, the amount of MS specifically captured by the test line region became higher (Figure 4f,g).

The basis for performance evaluation experiments was a series of documents from clinical and laboratory standards institute (CLSI). The evaluation results of linearity, precision and limit of detection were discussed below.

The strongly positive sample (32 ng/mL) and weakly positive sample (0.05 ng/mL) were mixed to obtain 7 concentrations (0.05, 5.4, 10.7, 16.1, 21.4, 26.7, and 32 ng/mL). Each sample was detected for three times and the average values were calculated. The average values and theoretical concentrations were linear fitted (Figure 5a, before aging) and the correlation coefficient (R) was higher than 0.99. This result indicated that there was a good linearity of this immunoassay platform in the range of 0.05–32 ng/mL.

Two concentration levels of cTnI were selected (0.5 and 8 ng/mL) and each sample was tested for 10 times, calculating the average value (M) and standard deviation (SD) respectively. CV was figured out to be 6.1% for 0.5 ng/mL and 8.0% for 8 ng/mL according to formula 1, both lower than 10%.

$$CV = SD/M \times 100\% \quad (1)$$

The cTnI free negative sample (0 ng/mL) was tested for 20 times, calculating the average value (M_{lot}) and standard deviation (SD_{lot}). According to the average values of negative and adjacent concentration sample, the two-point regression fitting equation was obtained (Figure 5b). The calculation result of $M_{lot} + 2SD_{lot}$ was plugged into the equation and the corresponding concentration was calculated to be 0.032 ng/mL, which was defined as the limit of detection.

After 30 days of heat aging test, the linearity curve became slightly lower (Figure 5a) but the R value was still higher than

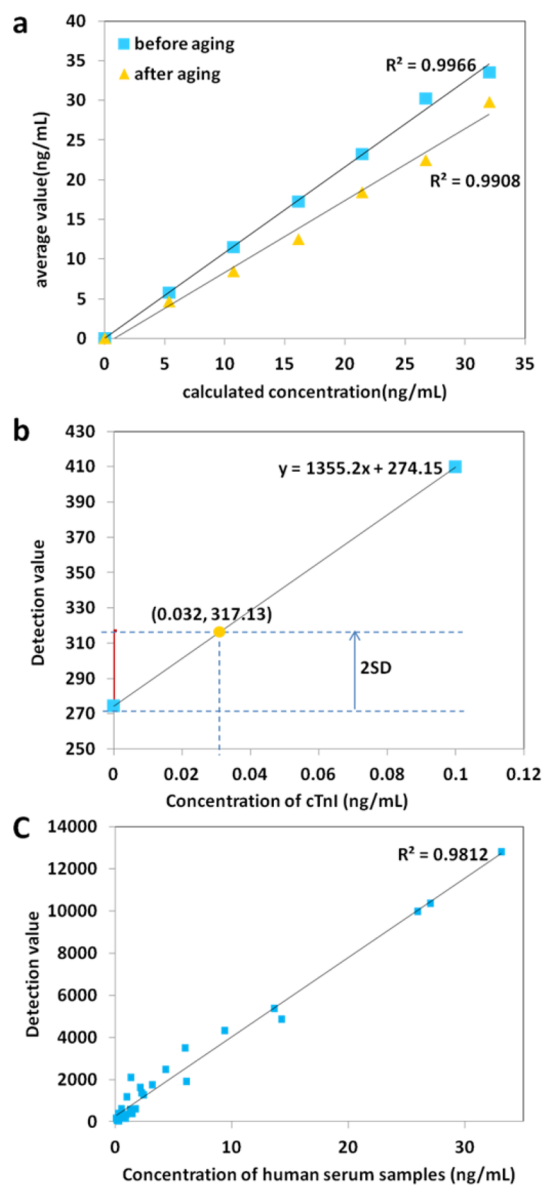


Figure 5. Performance evaluation of test strips: linearity before and after accelerated aging test (a); limit of detection (b); comparison with high-sensitivity commercial biochemical analyzer (c).

0.99. Besides, CV was 9.7% at 0.5 ng/mL and 8.6% at 8 ng/mL, both lower than 10%.

The human serum samples test results of lateral flow immunoassay platform and high-sensitivity commercial biochemical analyzer had a great correlation ($R > 0.99$), indicating that immunochromatography assay had a good accuracy in complex samples (Figure 5c).

In conclusion, in lateral flow immunoassay using fluorescent nanoprobes with oriented modified antibodies, the limit of detection could reach as low as 0.032 ng/mL in 15 min immunochromatography detection, showed good repeatability and stability, and correlated well with commercial instrument. The linearity was also great between 0.05 and 32 ng/mL, which meant the cTnI concentration in the range of 3 orders of magnitude could be detected and analyzed precisely, meeting the high demand of clinical application.

In comparison with biochemical analyzing platform, this study developed a simpler and faster detection method, with

much lower technical requirements for operators. Furthermore, the detection equipment was small, light, and portable. Last but not least, probes, antibodies, and other necessary reagents were all dried and immobilized on membranes, extending the validity period of test strips.

CONCLUSIONS

The antibody oriented modified probe construction technology developed in this research was superior to conventional passive adsorption, covalent coupling methods and simple SPG orientation methods without cross-linking reinforcement, which was extremely suitable for rapid detection to get more accurate results in a wide concentration range. This rapid, sensitive, and quantitative lateral chromatography platform was of great value to detect antigen markers requiring higher sensitivity, having broad application potential in disease diagnosis, food inspection, and environmental monitoring, especially suitable for point-of-care test. Since the detection values decreased a little after accelerated aging test for 30 days, in the future study, we will pay more attention to how to provide better, long-term protection for the immune activities of biological materials on membranes in a dry environment.

ASSOCIATED CONTENT

Supporting Information

The Supporting Information is available free of charge on the ACS Publications website at DOI: [10.1021/acs.analchem.7b05410](https://doi.org/10.1021/acs.analchem.7b05410).

Gradient cTnI detection results of different sizes of probes (0–32 ng/mL), gradient cTnI detection results of different sizes of probes (0–2 ng/mL), and gradient cTnI detection results with different probe preparation methods (PDF).

AUTHOR INFORMATION

Corresponding Authors

*E-mail: guning@seu.edu.cn (N. Gu). Tel.: +86-25-8327 2496-8005. Fax: +86-25 8327 2496.

*E-mail: zhangyu@seu.edu.cn (Y. Zhang). Tel.: +86-25-8327 2496-8005. Fax: +86-25 8327 2496.

ORCID

Ning Gu: [0000-0003-0047-337X](https://orcid.org/0000-0003-0047-337X)

Yu Zhang: [0000-0002-0228-7979](https://orcid.org/0000-0002-0228-7979)

Author Contributions

All authors have given approval to the final version of the manuscript.

Notes

The authors declare no competing financial interest.

ACKNOWLEDGMENTS

This work was supported by the National Key Research and Development Program of China (No. 2017YFA0205502); National Natural Science Foundation of China (Nos. 81571806 and 81671820); the Science and Technology Support Project of Jiangsu Province (No. BE2017763); the Jiangsu Provincial Special Program of Medical Science (No. BL2013029); and the Fundamental Research Funds for the Central Universities.

REFERENCES

(1) Orlov, A. V.; Bragina, V. A.; Nikitin, M. P.; Nikitin, P. I. *Biosens. Bioelectron.* **2016**, *79*, 423–429.

(2) Maltais, D.; Roy, R. L. *Environ. Toxicol. Chem.* **2007**, *26*, 1672–1676.

(3) Wang, Y.; Deng, R.; Zhang, G.; Li, Q.; Yang, J.; Sun, Y.; Li, Z.; Hu, X. J. *J. Agric. Food Chem.* **2015**, *63*, 2172–2178.

(4) Zhang, J.; Shen, Z.; Xiang, Y.; Lu, Y. *ACS Sens.* **2016**, *1*, 1091–1096.

(5) Liu, Y.; Jie, Y. *Microchim. Acta* **2016**, *183*, 1–19.

(6) Welch, N. G.; Scoble, J. A.; Muir, B. W.; Pigram, P. J. *Biointerphases* **2017**, *12*, 02D301.

(7) Fu, E.; Liang, T.; Houghtaling, J.; Ramachandran, S.; Ramsey, S. A.; Lutz, B.; Yager, P. *Anal. Chem.* **2011**, *83*, 7941–7946.

(8) Zhao, X.; Pan, F.; Garcia-Gancedo, L.; Flewitt, A. J.; Ashley, G. M.; Luo, J.; Lu, J. *J. R. Soc., Interface* **2012**, *9*, 2457–2467.

(9) Samanta, D.; Sarkar, A. *Chem. Soc. Rev.* **2011**, *40*, 2567–2592.

(10) Zhu, J.; Zou, N.; Zhu, D.; Wang, J.; Jin, Q.; Zhao, J.; Mao, H. *Clin. Chem.* **2011**, *57*, 1732–1738.

(11) Rao, S. V.; Anderson, K. W.; Bachas, L. G. *Microchim. Acta* **1998**, *128*, 127–143.

(12) Shen, M.; Rusling, J.; Dixit, C. K. *Methods* **2017**, *116*, 95–111.

(13) Baniukevic, J.; Kirlyte, J.; Ramanavicius, A.; Ramanaviciene, A. *Sens. Actuators, B* **2013**, *189*, 217–223.

(14) Del, M. G. M.; Villaverde, R.; Gonzalez-Rodriguez, I.; Vazquez, F.; Mendez, F. J. *Curr. Microbiol.* **2009**, *59*, 81–87.

(15) Brne, P.; Lim, Y. P.; Podgornik, A.; Barut, M.; Pihlar, B.; Strancar, A. *J. Chromatogr. A* **2009**, *1216*, 2658–2663.

(16) Wolfe, C. A. C.; Hage, D. S. *Anal. Biochem.* **1995**, *231*, 123–130.

(17) Liu, N.; Nie, D.; Tan, Y.; Zhao, Z.; Liao, Y.; Wang, H.; Sun, C.; Wu, A. *Microchim. Acta* **2017**, *184*, 1–7.

(18) Tajima, N.; Takai, M.; Ishihara, K. *Anal. Chem.* **2011**, *83*, 1969–1976.

(19) Clarizia, L. J.; Sok, D.; Wei, M.; Mead, J.; Barry, C.; McDonald, M. J. *Anal. Bioanal. Chem.* **2009**, *393*, 1531–1538.

(20) Treerattrakoon, K.; Chanthima, W.; Apiwat, C.; Dharakul, T.; Bamrungsap, S. *Microchim. Acta* **2017**, *184*, 1941–1950.

(21) Guss, B.; Eliasson, M.; Olsson, A.; Uhlen, M.; Frej, A.; Jornvall, H.; Flock, J.; Lindberg, M. *EMBO J.* **1986**, *5*, 1567–1575.

(22) Kronvall, G.; Seal, U. S.; Finstad, J.; R, W., Jr. *J. Immunol.* **1970**, *104*, 140–147.

(23) Kwon, Y.; Han, Z.; Karatan, E.; Mrksich, M.; Kay, B. K. *Anal. Chem.* **2004**, *76*, 5713–5720.

(24) Bereli, N.; Ertürk, G.; Tümer, M. A.; Say, R.; Denizli, A. *Biomed. Chromatogr.* **2013**, *27*, 599–607.

(25) Makaraviciute, A.; Ramanaviciene, A. *Biosens. Bioelectron.* **2013**, *50*, 460–471.

(26) Dubrovsky, T.; Tronin, A.; Dubrovskaya, S.; Guryev, O.; Nicolini, C. *Thin Solid Films* **1996**, *284–285*, 698–702.

(27) Ryu, Y.; Jin, Z.; Kang, M. S.; Kim, H. S. *BioChip J.* **2011**, *5*, 193–198.

(28) Anderson, G.; Scott, M. *Clin. Chem.* **1991**, *37*, 398–402.

(29) Wang, C.; Food, S. *China Medical Device Information* **2008**, *5*, 67–70.

(30) Akerström, B.; Björck, L. *J. Biol. Chem.* **1986**, *261*, 10240–10247.

(31) Ward, G.; Mckinnon, L.; Badrick, T.; Hickman, P. E. *Am. J. Clin. Pathol.* **1997**, *108*, 417–421.

(32) Björck, L.; Kronvall, G. *J. Immunol.* **1984**, *133*, 969–974.